Rev.Adv.Mater.Sci. 5 (2003) 481-486

MICROSTRUCTURE OF Fe NANOPARTICLES FABRICATED BY CHEMICAL VAPOR CONDENSATION

Taek-Soo Kim[1], Wei Sun[2], Chul-Jin Choi[3] and Byong-Taek Lee[1]

[1]School of Advanced materials Engineering, Kongju National University, Kongju, Chungnam, 314-701, Korea
[2]Institute for Materials Research, Tohoku University, Katahira 2-1-1, Aoba-ku, 980-8577 Sendai, Japan
[3]Korea Institute of Machinery and Materials, Changwon, Kyungnam, 641-010, Korea

Received: July 26, 2003

Abstract. Iron and Iron nitride nanoparticles were synthesized by chemical vapor condensation (CVC) process, using a precursor of $Fe(CO)_5$ and carrier gas of NH_3. The crystallization behaviors were examined using X-Ray Diffractometry (XRD) and Transmission Electron Microscopy (TEM) technique. α-Fe nanoparticles were found to form at a lowest decomposition temperature of 500 °C. As the temperature increased up to 700 °C, the crystallization of α-Fe phases was suppressed, and Fe_3N nanoclusters less than 5 nm in diameter were begun to form. Further increase of the decomposition temperature enriched Fe_3N region by the phase; the complete crystallization of Fe_3N was observed at 1000 °C. Typical particle size of the α-Fe and Fe_3N particles was approximately 30~40 nm in diameter.

1. INTRODUCTION

Nanopowder is usually defined as a powder consisting of the extremely fine particles with the diameter less than 100 nm. The research in this field has been explosively conducted [1,2] due to the fact that nanomaterials posses a number of innovatively anticipated properties, which can not be obtained from conventional bulk materials [2,3]. As compared with the bulk materials, nanoparticles present a quite distinctive physical and chemical properties, which give rise to innovative mechanical properties [3]. Thus, nanomaterials may significantly enhance the area of materials application that is now limited by the properties of existent materials [4].

In order to fabricate the nanoparticles, vaporization method has been frequently used, in which the target materials are vaporized by heat source and then rapidly condensed. The vaporization processes can be subdivided into physical and chemical ones depending on the reaction [5,6]. If the resultant nanoparticles have the same composition with the target materials, it is prepared by physical vapor condensation (PVC) [7]. However, nanoparticles having a different composition with the target are usually obtained by chemical vapor condensation (CVC), because the chemical reaction occurs between the vapor and other system components during the vaporization and condensation [8,9]. The CVC process has a merit in selecting composition, whereas the PVC in purity [9].

In this investigation, CVC process was used to fabricate the Fe or Fe_3N nanoparticles, which are known to show an excellent magnetic property and corrosion resistance as well as a good mechanical property [10]. The use of $Fe(CO)_5$ precursor and NH_3 carrier gas gives an opportunity to change the phase of these nanoparticles (Fe and Fe_3N) during the CVC process. This work focuses on the study of the variations in composition and phases of the resultant nanoparticles during the CVC process with the precursor decomposition temperature.

Corresponding author: Taek-Soo Kim, e-mail: taeksoo@kongju.ac.kr

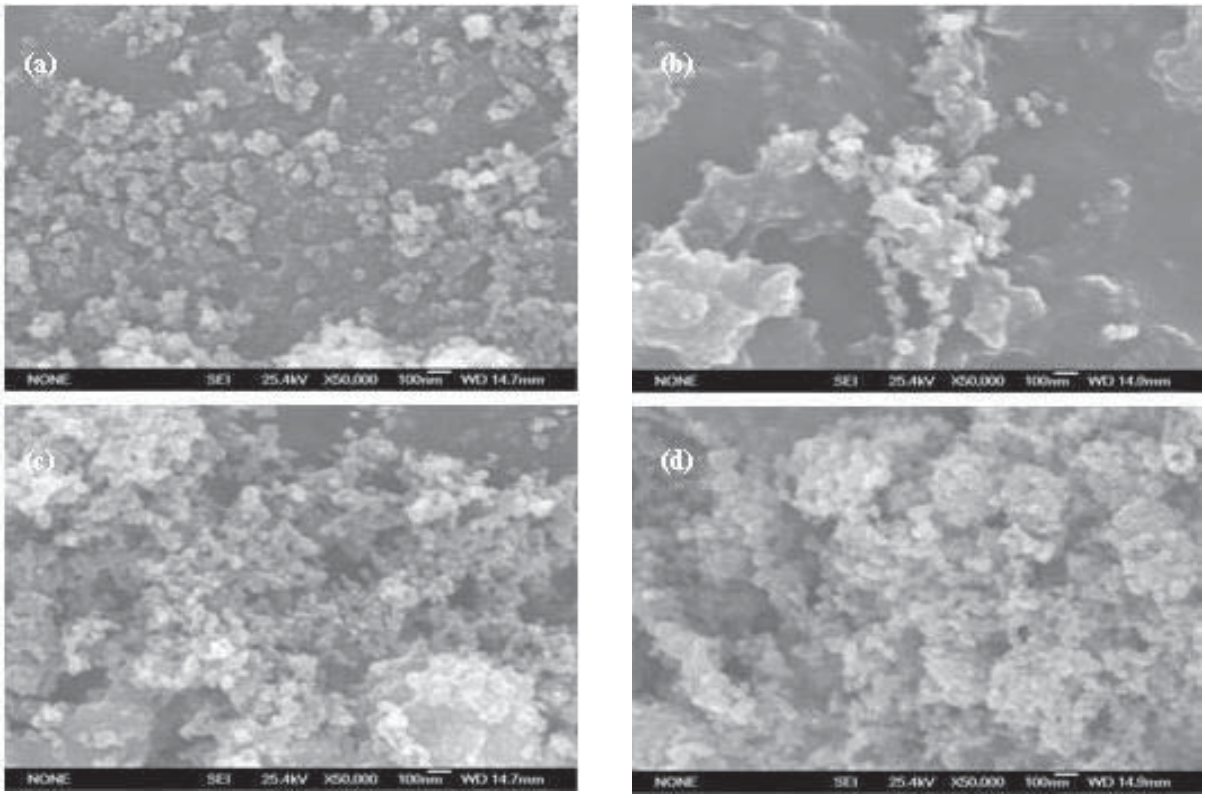

Fig. 1. SEM microstructure of Fe/N nano powders (a) 500 °C, (b) 700 °C, (c) 900 °C, (d) 1000 °C.

2. EXPERIMENTAL

Fe based nanoparticles were produced using CVC process. The metal vapor was generated by the heating of $Fe(CO)_5$ precursor, this vapor was then rapidly condensed in a cold chamber with the temperature controlled by liquid N_2 [11,12]. In order to carry the vapor into the cold chamber, NH_3 was used as a carrier gas. Chemical reaction between the Fe vapor and nitrogen in the carrier gas occurred during the movement. The CVC system had a closed circuit and was evacuated down to 1 Torr using a conventional rotary pump. The flow rates of the precursor and the carrier gas were 350.0 sccm and 2.0 sccm, respectively. In order to study the effect of the decomposition temperature on the nanoparticle phases, $Fe(CO)_5$ was pyrolyzed at temperatures of 500 °C, 700 °C , 900 °C, and 1100 °C.

Morphology examination and phase characterization of the nanoparticles were conducted by Scanning Electron Microscopy (SEM; JSM6335F) and XRD (Rigaku, AX-2500), respectively. Microstructure of the nanoparticles was examined using TEM (JEM2010) and High Resolution TEM (HTTEM; JEM4000EX). In order to prepare the TEM specimen, nanoparticles were mixed with G1 epoxy and cut into a disc using a microtome.

3. RESULTS AND DISCUSSION

Figs.1a-1d show the SEM morphologies of the Fe nanoparticles decomposed from the $Fe(CO)_5$ precursor at decomposition temperatures of 500 °C, 700 °C, 900 °C, and 1000 °C, respectively. It is seen that the nanoparticles had a relatively spherical shape, but most of them were agglomerated, regardless of the decomposition temperature. An average particle size of the nanoparticles is almost similar and equals ~ 30-40 nm in diameter. In order to characterize the variation in the phases with decomposition temperature in detail, XRD studiy was conducted; the results are presented in Fig. 2. The nanoparticles were shown to consist of α-Fe only at 500 °C, but a broad halo formed along the Fe main diffraction peak of (110) indicates a partial distribution of α-Fe on the existent amorphous phase (Fig. 2a). As the decomposition temperature was increased up to 900 °C and 1000 °C, the main phase was observed to turn into a Fe_3N (Figs. 2c and 2d). However, no diffraction peak attributed to crystalli-

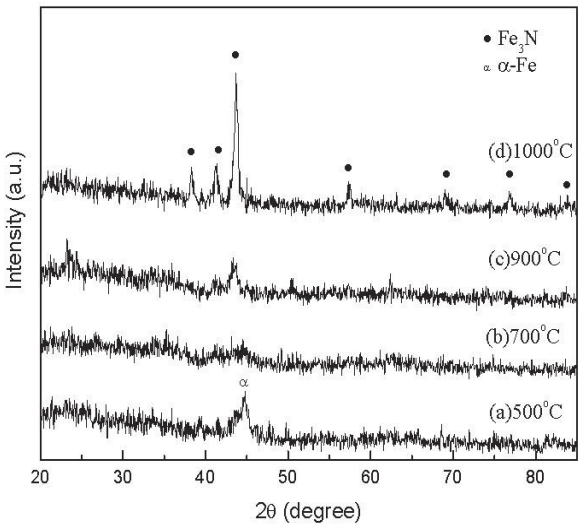

Fig. 2. XRD characterization of Fe-N nanoparticles with the decomposition temperature of (a) 500 °C, (b)700 °C, (c) 900 °C, (d)1000 °C.

zation was registered at 700 °C; this fact indicates that the crystallization of both α-Fe and Fe_3N was suppressed (Fig. 2b). Similar to the solidification of metals, the condensation process may be absolutely dependent on the cooling rate and composition during the CVC process [7,13]. It is thought that the condensation rate from the vapor to solid is practically the same throughout this process, since $Fe(CO)_5$ precursor was completely evaporated at temperatures over 400 °C and condensed under liquid N_2 environment. Thus, the formation of the different phases at the decomposition temperatures studied may be attributed to the variations in the vapor composition, i.e. in the percentage of the precursor vapor and the carrier gas. The increase in the decomposition temperature give rise to the increase of the Fe vapor pressure, while the pressure of the nitrogen vapor remains constant. In addition, the elevated temperature is enough to provide the activation energy for reaction between Fe and N atoms. Thus, we believe Fe-N compound to be formed due to the gaseous reaction at a certain temperature. The ratio of the vapor concentration of the both elements and the activation energy for their reaction at 700 °C are slightly higher than those at 500 °C, so the leading phases have a short range order. For this reason, the crystallization peak was not observed at these temperatures (Fig. 2b). As the decomposition temperature increases up to 900 °C, the formation of the Fe_3N particles starts on the existent amorphous matrix, because of the values

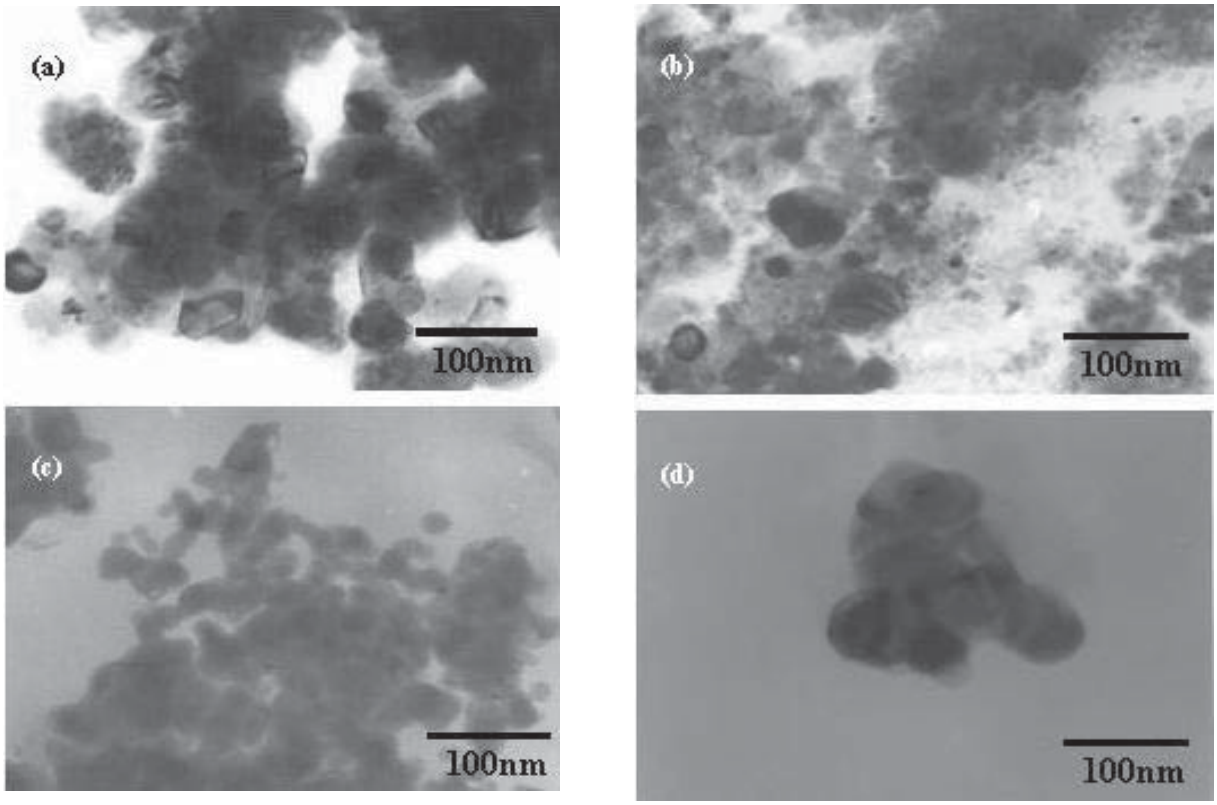

Fig. 3. TEM microstructure of Fe-N nanoparticles with decomposition temperature of (a) 500 °C, (b) 700 °C, (c) 1000 °C, (d) 900 °C.

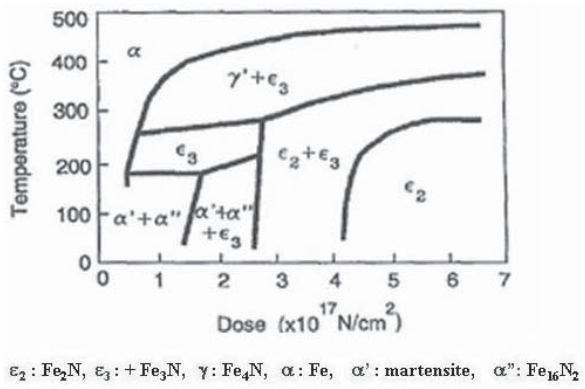

Fig. 4. Phase map for Fe-N with N contents.

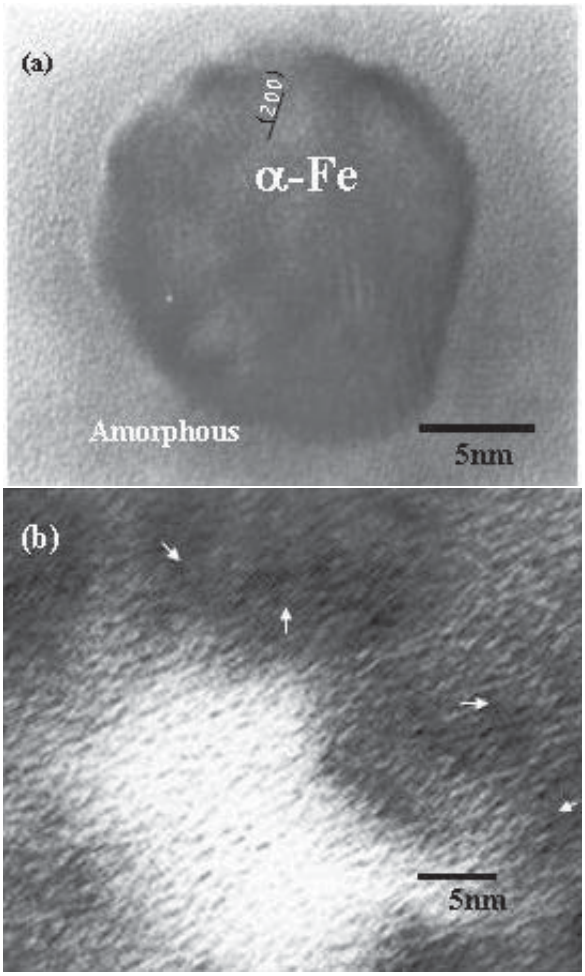

Fig. 5. TEM microstructure of Fe-N nano powders decomposed at 700 °C. (a) a-Fe partially formed and (b) Fe_3N nanoparticles taken from an amorphous area in Fig. 5a.

of the activation energy and vapor concentrations provides the possibility for the reaction. With the temperature increasing up to 1000 °C, further crystallization has occurred from the remained amorphous phase, and, finally, all phase will consist of Fe_3N nanoparticles. To sum up, variation in the vapor composition and activation energy during the CVC process induces a difference in the resultant phases, resulting in that Fe or Fe_3N rich crystals, which are formed at temperatures lower or higher than 700 °C, respectively.

Figs. 3a-3d show the TEM microstructure of the changes in Fe or Fe_3N nanoparticles with the decomposition temperature. The size of the nanoparticles is quite similar to that examined by SEM (Fig.1), but the particles with the diameters less than 20 nm are observed here. These particles are formed in the amorphous matrix taken from the specimen decomposed at 700 °C. However, the average size increases to be about 40 nm in diameter at 1000 °C. This fact agree with the data that the size of nanoparticle prepared by CVC becomes coarse with the increase in the decomposition temperature [7,13] due to the increase in the metal vapor concentration [7,13]. But these ideas may be more effective for the case of an inert gas (Ar and Ne) used as the carrier gas. This is due to the fact that the inert gas does not react with the metal vapor, and there will not be a stoichiometric change in the gas composition with the decomposition temperature. On the other hand, the size of Fe_3N particles may not be coarsen without the simultaneous increase in Fe and N concentrations. Indeed, the increase in the decomposition temperature leads to the increase in Fe vapor pressure, while the nitrogen pressure remains constant. Thus, further formation of Fe_3N compound will not occur, but the composition of the resultant compound will be shifted into the Fe rich region like Fe_4N (an example is shown in Fig. 4 [14]). The analysis of the Fe-N equilibrium phase diagram indicates that $Fe_{16}N$ can form at the lowest N concentration; on the contrary, Fe_2N compound is preferable in the N-rich area [14]. It is also noted that a shift in the temperature and concentration results in the formation of some other Fe-N compounds such as Fe_4N and Fe_3N.

Fig. 5 is a HRTEM microstructure of the Fe/N nanoparticles decomposed at 700 °C. It is seen that α-Fe less than 20 nm in diameter was crystallized in the amorphous matrix (Fig. 5a). In addition, very fine clusters with Fe_3N composition and the diameter less than 5 nm are distributed throughout the Fe-N amorphous matrix (Fig. 5b). These combined particle distribution at 700 °C may be due to the fact that the temperature becomes closer to a preferential condition for Fe_3N formation. HRTEM mi-

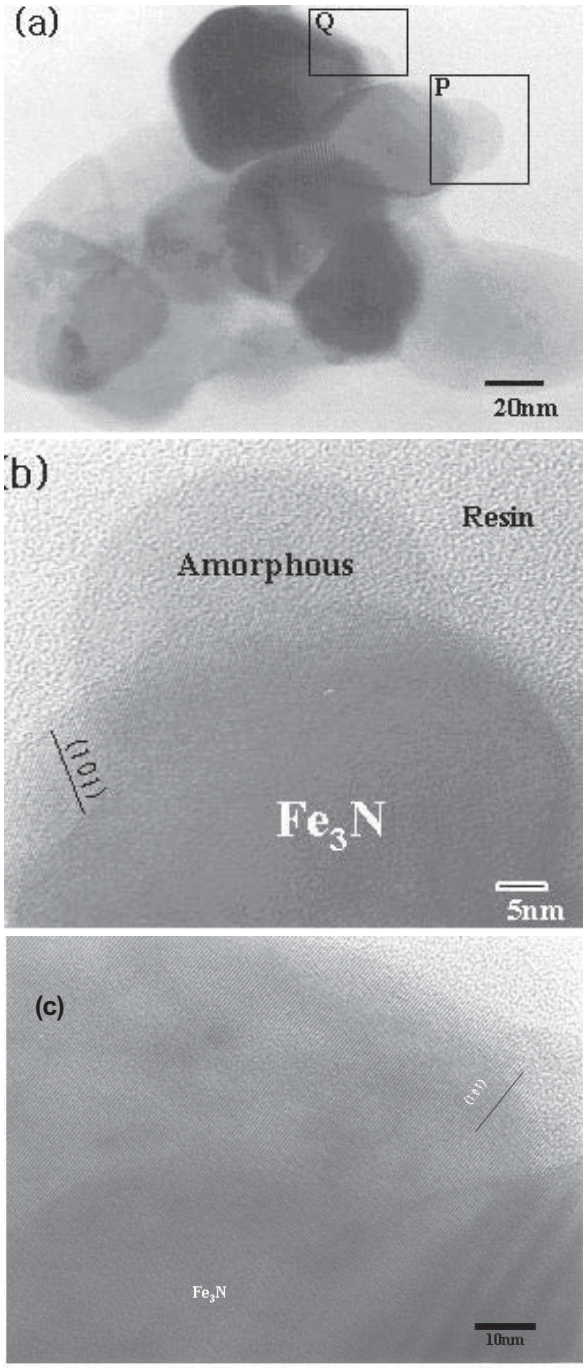

Fig. 6. TEM microstructure (a) of Fe-N nanopowders decomposed at 1000 °C and the enlarged image (b) and (c) taken from P) and Q) of Fig.6a, respectively.

crostructure of the particles decomposed at 1000 °C is shown in Fig. 6. Two types of nanoparticles having amorphous and crystalline phases can be seen in Fig. 6b, which is enlarged from *P* area of Fig. 6a. The Fe_3N particles are about 40 nm in diameter, while the amorphous particles are less than 20 nm. It is generally understood that the cooling or condensation rate affect the resultant particle size during the condensation and rapid solidification. Thus, the smaller particle experienced a rapid condensation rate rather than the coarse particles, resulting in a formation of the amorphous phase. Fig. 6c magnified from *Q* area in Fig.6a shows a typical Fe_3N nanoparticles having (101) crystal plane.

4. CONCLUSION

Fe and Fe_3N nanoparticles with an average particle size of 30-40 nm in diameter were successfully fabricated using CVC process. The concentration of the Fe vapor and the activation energy for reaction between Fe and N atoms increased with the decomposition temperature, resulting in a various crystallization sequence. Decomposition at 500 °C forms Fe nanoparticles embedded in amorphous matrix, but almost amorphous phase is produced at 700 °C. The fractions of Fe nanoparticles with the typical size less than 40 nm and Fe_3N clusters with the size less than 5nm are distributed in the amorphous matrix at 700 °C. The complete Fe_3N crystallization as well as a coarsening of the particles occurs at temperatures as high as 1000 °C.

ACKNOWLEDGEMENTS

This research was performed by the financial support of 'Center for Nanostructured Materials Technology' under '21st Century Frontier R&D Programs' of the Ministry of Science and Technology, Korea and also partially supported by the 2002 NRL research program of Korean Ministry of Science and Technology.

REFERENCES

[1] Y.Chen, N.Glumac, B.H.Kear and G.Skandan // *Nanostruc. Mater.* **9** (1997) 101.
[2] Z.H.Wang, C.J.Choi, B.K.Kim and Z.D.Zhang // *Mater. Lett* (2003), in press.
[3] A.S.Edelstein and R.C.Cammarata, *Nanomaterials Synthesis, Properties and Appliction* (Institute of Physics Publishing, London, 15, 1996).
[4] C.J.Choi and B.K.Kim // *J.Kor.Inst.Met. & Mater.* **40** (2002) 711.
[5] W.Jiang and K.Yatsui // *IEEE Trans. on Plasma Sci.* **26** (1998) 1498.
[6] Y.Champion, S.Guerin-Mailly, J.-L.Bonnentien and P.Langlois // *Scrip. Mater.* **44** (2001) 1609.
[7] P.G.Sanders, J.A.Eastman and J.R.Weertman // *Acta Mater.* **45** (1997) 4019.

[8] C.J.Choi, O.Tolochko and B.K.Kim // *Mater. Lett.* **56** (2002) 289.
[9] W.Chang, G.Skandan, S.C.Danforth, B.H.Kear and H.Hahn // *Nanostruct. Mater.* **4** (1994) 507.
[10] Z.Q.Yu, J.R.Zhang and Y.W.Du // *J. Magne. and Magnetic Mater.* **159** (1996) L8.
[11] B.K.Kim and C.J.Choi // S*crita Mater.* **44** (2001) 2161.
[12] J.P.Ahn, J.K.Park and M.Y.Huh // *J.Kor.Inst.Met. & Mater.* **34** (1996) 877.
[13] A.Singhal, G.Skandan, N.Glumac and B.H.Kear // *Scripta Mater.* **44** (2001) 2203.
[14] M.Kopcewicz and J.Jagielski // *J Appl. Phys.* **71** (1992) 4217.